Quantum Chemical Study on Enantioselective Reduction of Aromatic Ketones Catalyzed by Chiral Cyclic Sulfur-Containing Oxazaborolidines. Part 1. Structures and Properties of Catalysts

MING LI,* RUGANG XIE, CHANGWEI HU, XIN WANG, ANMIN TIAN

Department of Chemistry, Sichuan University, Chengdu 610064, People's Republic of China

ABSTRACT: The ab initio molecular orbital method is employed to study the structures and properties of chiral cyclic sulfur-containing oxazaborolidine, as a catalyst, and its borane adducts. All the structures are optimized completely by means of the Hartree–Fock method at 6-31g* basis sets. The catalyst is a twisted chair structure and reacts with borane to form four plausible catalyst–borane adducts. Borane–sulfur adducts may be formed, but they barely react with aromatic ketone to form catalyst–borane–ketone adducts, because they are repulsed greatly by the atoms arising from the chair rear of the catalyst with a twisted chair structure. Borane–N adduct has the largest formation energy and is predicted to react easily with aromatic ketone to form catalyst–borane–ketone adducts. The formation of the catalyst–borane adducts causes the B_{BH3}—H_{BH3} bond lengths of the BH_3 moiety to be increased and thus enhances the activity of the enantioselective catalytic reduction. The borane–N adduct is of great advantage to hydride transfer.   © 2000 John Wiley & Sons, Inc. Int J Quant Chem 78: 245–251, 2000

**Key words:** ab initio; cyclic sulfur-containing oxazaborolidine; enantioselective reduction; catalyst–borane adduct

Introduction

In recent years, a new type of oxazaboro-lidines—chiral cyclic sulfur-containing oxaza-borolidines—has been synthesized and used as an effective catalyst in the enantioselective catalytic reduction of ketone [1–4]. Because chiral cyclic sulfur-containing oxazaborolidine catalysts were reported first by Li and Xie [1], Huang et al. [2], Reiners et al. [3], and Trentmann et al. [4], respectively, they are called for the purpose of convenient discussion, the Chengdu–Taipei–Oldenburg (CTO) catalysts herein. The CTO catalyst **1** is obtained by replacement of pyrrolidine with thiazolidine in the CBS catalyst **1a**. In general, when the oxazaboro-lidine **1a**, which is of an S-chirality at the C4 site, is used in the enantioselective reduction of aromatic ketone with borane, (R) alcohols are obtained. However, when the enantioselective reduction of aromatic ketone is catalyzed by the CTO **1** arising from the (4S)-CBS **1a**, (S) alcohols, not (R) alcohols, are generated. This is a significant work not only for synthetic chemistry, but also for theoretical chemistry. The CTO catalysts are of importance in the enantioselective catalytic reduction of ketone.


1a   **1**
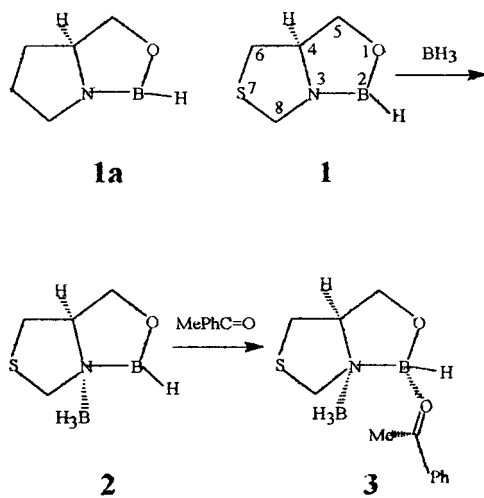
The mechanism of the enantioselective reduction catalyzed by the CBS catalysts was suggested by Corey et al. [5]. According to this mechanism of catalysis, the enantioselective reduction of aromatic ketone catalyzed by the CTO catalysts mainly involves the following steps: formation of the CTO–borane adduct **2**; coordination of aromatic ketone to

be reduced to the adduct **2**, leading to the CTO–borane–ketone adducts **3**; hydride transfer from the borane moiety to the carbonyl carbon in the adducts **3** followed by a number of regenerative steps. The reduced products are the chiral alcohols $R_L R_S C(OH)H$. The ab initio molecular orbital calculations about the CBS catalyst **1a** and its borane adduct at the N site were carried out by Nevalainen [6]. However, ab initio studies on the CTO catalyst and on the enantioselective reduction catalyzed by CTO have not been reported yet. Therefore, the aim of this work is to investigate the structure of the CTO catalyst and its catalytic properties with the ab initio molecular orbital method.

Computations and Results

For all the computed systems, standard ab initio molecular orbital basis sets 6-31g* are used. When borane reacts with the CTO catalyst **1**, it may coordinate at the O(1), N(3), or S(7) site. As a result, the reaction of borane with the CTO catalyst **1** may lead to five different structures of CTO–borane adducts. All the plausible structures of the CTO–borane adducts are shown in Scheme 1, where the structures in which borane coordinates at the O(1) site have two plausible conformations, such as **2-1a** and **2-1a'**, the structures in which borane coordinates at the S(7) site also have two different conformations, such as **2-1b** and **2-1b'**, and borane in the structure **2-1c** coordinates at the N(3) site. The CTO catalyst **1** and all the structures of the CTO–borane adducts are optimized completely by means of the Hartree–Fock method at 6-31g* basis sets with program Gaussian 92. The optimized structures are illustrated in Figures 1 and 2, respectively. The selected atomic charges are given in Table I. For all the structures, total energies, formation energies, dipole moments, and selected bond lengths are summarized in Table II. Mulliken overlap populations, which are given in parentheses, are also summarized in Table II. The selected energy levels of valence natural atomic orbitals from the natural bond orbital (NBO) analysis and the selected stabilization interaction energies $E(2)$ obtained from the second-order perturbative theory [7, 8] are listed in Tables III and IV, respectively. The results for the CTO catalyst **1** are also listed in these tables.

2   **3**
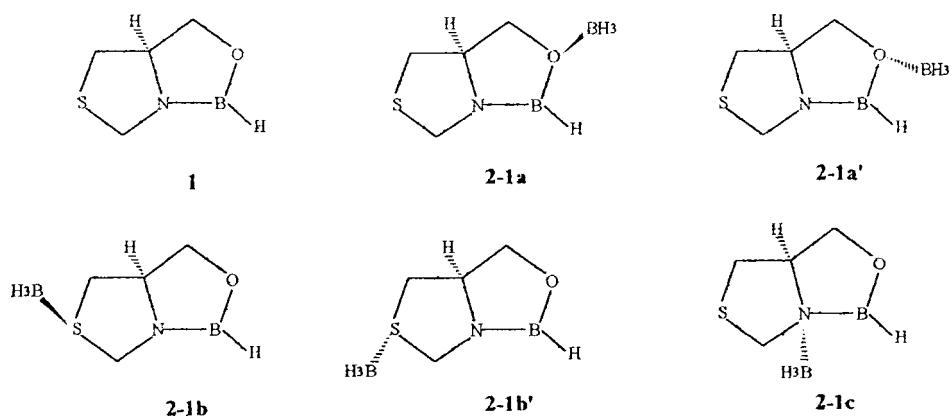
SCHEME 1.

Discussion

THE CTO CATALYST

The optimized structure of the CTO catalyst **1** is shown in Figure 1. Its dipole moment D and total energy E are 1.71 D and −707.7065 au, respectively (see Table II). The vibrational analysis of the CTO catalyst **1** is also carried out by means of the Hartree–Fock method at 6-31g* basis sets. The value of the lowest vibrational frequency is 88.96 cm^{-1}, which implies that the optimized structure of the CTO **1** is stable (a structure is stable if it has no imaginary frequencies). As presented in Figure 1, the CTO catalyst **1** is a twisted chair structure. The C(6)–C(4)–N(3)–B(2) and C(8)–N(3)–C(4)–C(5) torsion angles are 105.6 and 168.0°, respectively. The B(2)—N(3) bond length is 1.415 Å, and the lengths of the N(3)—C(4) and N(3)—C(8) bonds are, re-
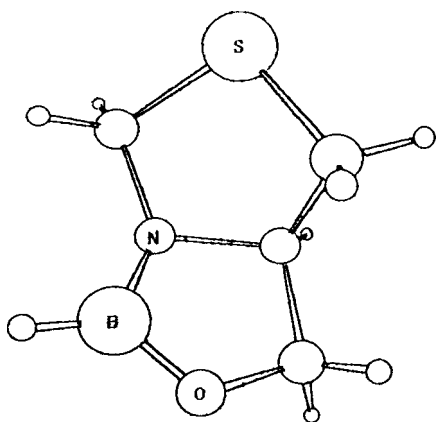
spectively, 1.452 and 1.430 Å. There is a partial π bond between O(1) and B(2). The O(1)—B(2) bond length is 1.361 Å. The C(5)–O(1)–B(2), O(1)–B(2)–N(3), B(2)–N(3)–C(4), and N(3)–C(4)–C(5) angles are 109.6, 110.5, 108.3, and 102.3°, respectively. The S(7)—C(6) and S(7)—C(8) bond lengths are 1.825 and 1.852 Å, and the C(6)–S(7)–C(8) angle is 92.89°. In addition, the B(2)—H length is 1.184 Å, and H, O(1), B(2), and N(3) atoms are located on almost the same plane. Obviously, the O(1)—B(2) partial π bond is formed by the overlap of an empty p orbital of B(2) with the lone pairs of O(1).

It is seen from Table I that the net charges for O(1), B(2), N(3), and S(7) atoms are −0.624, 0.593, −0.626, and 0.102, respectively. Seemingly, O(1) and N(3) may coordinate easily with hydrions or atoms that lack electrons, such as B in borane, because of their large negative charges. However, the trend of the O(1) atom as a donor, donating electrons to borane, is weak because of its great electronegativity. Therefore, borane coordinates easily at the N(3) site. For the soft Lewis base S(7), according to the rule of hard–soft acids and bases proposed by Pearson [9], it may coordinate with the soft Lewis acid BH$_3$. Since it has a positive charge, however, the trend of S(7) donating electrons to borane is also weak. These results imply that borane coordinates before hand at the N(3) site. This may also be concluded with the energy levels of valence natural atomic orbitals from the NBO analysis [7, 8]. It is clear from Table III that among the O(1), N(3), and S(7) atoms, the valence orbital levels of the O(1) atom are the lowest. Since the B$_{BH3}$ of borane has high valence orbital levels as an electron acceptor, the energy differences between the valence levels of O(1) and B$_{BH3}$ are the largest, which results in the smallest orbital interactions and

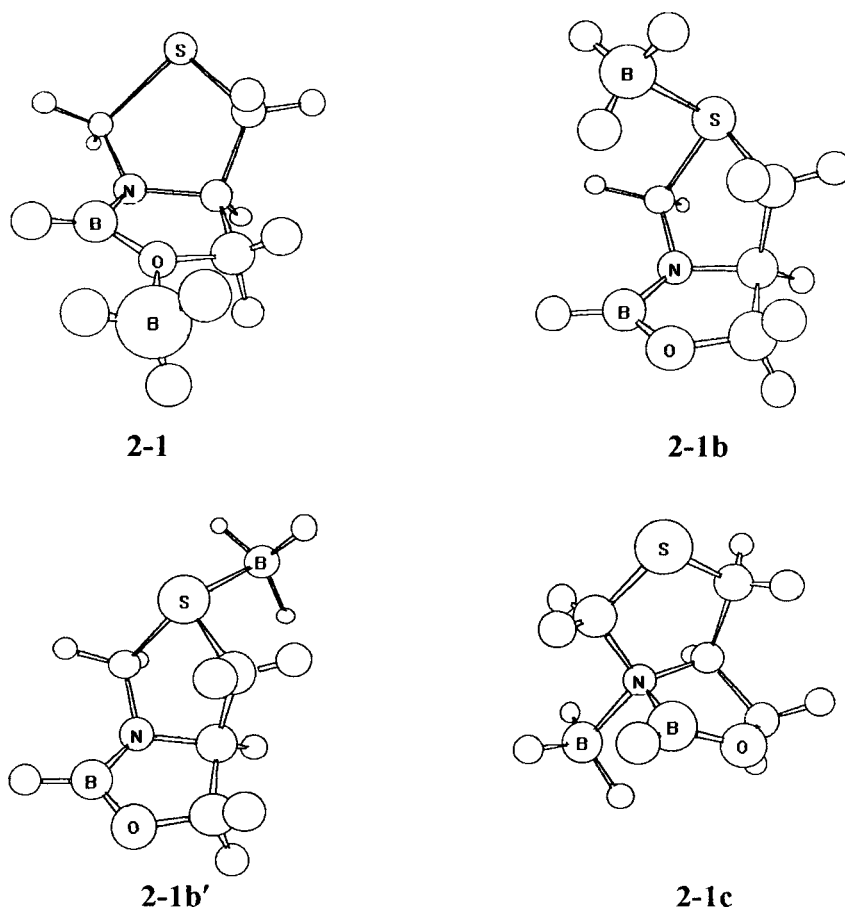**FIGURE 1.** Optimized structures of the CTO catalyst.

FIGURE 2. Optimized structures of the CTO–borane adducts.

in a small electron transfer. The natural charge of S(7) is 0.168, which is obviously of no advantage to the transfer of electrons from S(7) to the B_{BH3} of borane. Therefore, the coordination of borane to N(3) is prior. Of course, it must be emphasized that the formation of the borane–O adduct and the borane–sulfur adducts cannot be excluded absolutely in the enantioselective reduction.

THE CTO–BORANE ADDUCTS

The optimized structures for the CTO–borane adducts are illustrated in Figure 2. It is revealed that two plausible conformations for the coordination of borane at the O(1) site, **2-1a** and **2-1a′** shown in Scheme 1, are turned into the same structure as **2-1** illustrated in Figure 2, after being optimized

TABLE I

Selected atomic charges for CTO–borane adducts.

	O(1)	B(2)	N(3)	S(7)	B_{BH3}	BH_3
2-1	−0.680	0.617	−0.623	0.126	0.201	−0.140
2-1b	−0.617	0.610	−0.626	0.306	−0.049	−0.308
2-1b′	−0.619	0.593	−0.628	0.306	−0.052	−0.316
2-1c	−0.591	0.682	−0.730	0.145	0.098	−0.225
CTO	−0.624	0.593	−0.626	0.102		
BH_3					0.115	

TABLE II

Dipole moments D (D), total energies E (au), formation energies ΔE (kJ/mol), selected bond lengths (Å), and selected Mulliken overlap populations (in parentheses) for the CTO–borane adducts.

	2-1	2-1b	2-1b′	2-1c	CTO	BH_3
D	4.30	5.24	3.14	3.91	1.71	
E	−734.1078	−734.1097	−734.1106	−734.1133	−707.7065	−26.3893
ΔE	−31.48	−36.63	−38.91	−45.87		
B_{BH3}—H_{BH3}	1.197	1.202	1.201	1.210		1.188
	(0.417)	(0.415)	(0.415)	(0.414)		(0.413)
B(2)—N(3)	1.389	1.359	1.358	1.496	1.414	
	(0.336)	(0.409)	(0.410)	(0.309)	(0.443)	
N(3)—B_{BH3}				1.717		
				(0.118)		
O(1)—B_{BH3}	1.751					
	(0.061)					
S(7)—B_{BH3}		2.080	2.073			
		(0.192)	(0.197)			

completely. In the structure **2-1**, B_{BH3}, O(1), B(2), and C(5) atoms are on the same plane. As presented in Table II, among all the structures of the CTO–borane adducts, the structure with the largest formation energy is **2-1c**. For four structures of the CTO–borane adducts, the formation energies, ΔE, are **2-1**, −31.48 kJ/mol; **2-1b**, −36.63 kJ/mol; **2-1b′**, −38.91 kJ/mol; **2-1c**, −45.87 kJ/mol. The formation reaction of the CTO–borane adducts is exothermic. From the point of view of energy, it is clear that the coordination of borane at the N(3) site is of great advantage to the formation of the CTO–borane adducts.

It is clear from Table I that for each of the structures, the BH_3 moiety has a negative charge (**2-1**, −0.140; **2-1b**, −0.308; **2-1b′**, −0.316; **2-1c**, −0.225), which implies that electrons transfer from CTO to the BH_3 moiety. For the borane–O adduct **2-1**, because of its great electronegativity, the trend of the O(1) atom, as a donor of electrons to the BH_3 moiety, is weak although it has a great negative charge. For the borane–sulfur adducts **2-1b** and **2-1b′**, the positive charges of S(7) are increased from 0.102 for CTO to 0.306 for the adducts, increasing by 0.204. Obviously, electrons transfering to the BH_3 moiety are mainly due to S(7). Since the charges of S(7) are positive, the transfer of electrons from S(7) to the BH_3 moiety must lead to an increase in energy, which is of no advantage to the stability of the systems. This result is in correspondence with the high energies of the borane–sulfur adducts. In the borane–N adduct **2-1c**, the coordination of borane at the N(3) site re-

sults in a great increase in the negative charge of N(3), from −0.626 for CTO to −0.730 for **2-1c**. The increase in the negative charge of N(3) causes the interaction between the CTO catalyst and borane to be strengthened, which is advantageous to the stabil-

TABLE III

Energy levels of valence natural atomic orbitals E (au) for the CTO–borane adducts.

	Atom	Type	E	Type	E
2-1	B(2)	s	0.1521	px	0.3034
		py	0.3158	pz	0.1815
2-1b	B(2)	s	0.1672	px	0.2589
		py	0.3388	pz	0.2429
2-1b′	B(2)	s	0.1623	px	0.3023
		py	0.3249	pz	0.1911
2-1c	B(2)	s	0.1192	px	0.1856
		py	0.2821	pz	0.3092
CTO	O(1)	s	−1.1442	px	−0.4975
		py	−0.4006	pz	−0.4440
	B(2)	s	0.1791	px	0.3037
		py	0.3254	pz	0.2343
	N(3)	s	−0.6598	px	−0.3257
		py	−0.2674	pz	−0.3659
	S(7)	s	−0.8454	px	−0.2042
		py	−0.1205	pz	−0.3212
BH_3	B	s	−0.0474	px	0.1581
		px	0.1957	pz	0.1957
MePhC=O	O	s	−1.1189	px	−0.4351
		py	−0.4351	pz	−0.2814

TABLE IV
Selected stabilization interaction energies $E(2)$ (kcal/mol) for CTO–borane adducts.

		Donor NBO		Acceptor NBO	$E(2)$
2-1	BD	B_{BH3}—H_{BH3}	BD*	O(1)—B(2)	0.68
	BD	B_{BH3}—H_{BH3}	BD*	O(1)—B_{BH3}	3.04
	LP	O(1)	BD*	B_{BH3}—H_{BH3}	1.28
2-1b	BD	B_{BH3}—H_{BH3}	BD*	S(7)—B_{BH3}	2.42
	LP	S(7)	BD*	B_{BH3}—H_{BH3}	0.69
2-1b'	BD	B_{BH3}—H_{BH3}	BD*	S(7)—B_{BH3}	2.34
	LP	S(7)	BD*	B_{BH3}—H_{BH3}	0.79
2-1c	BD	B_{BH3}—H_{BH3}	BD*	N(3)—C(8)	1.81
	BD	B_{BH3}—H_{BH3}	BD*	B(2)—N(3)	0.66
	BD	B_{BH3}—H_{BH3}	BD*	N(3)—B_{BH3}	0.96
	BD	B_{BH3}—H_{BH3}	BD*	O(1)—B(2)	4.39
BH_3	BD	B(1)—H(2)	BD*	B(1)—H(3)	0.53
	BD	B(1)—H(2)	BD*	B(1)—H(4)	0.53

ity of the borane–N adduct **2-1c**. It is obvious from these discussions that borane coordinates easily at the N(3) site to form the borane–N adduct **2-1c**.

In the CTO catalyst **1**, the positive charge of B(2), $Q_{B(2)}$, is 0.593. After the forrnation of the CTO–borane adducts, $Q_{B(2)}$ are **2-1**, 0.617; **2-1b**, 0.610; **2-1b'**, 0.593; **2-1c**, 0.682. Notice that $Q_{B(2)}$ for the borane–sulfur adducts **2-1b** and **2-1b'** hardly changes and that the variation in $Q_{B(2)}$ for the borane–O adduct **2–1** is also small. $Q_{B(2)}$ for the borane–N adduct **2-1c** increases by about 0.09. Obviously, the Lewis acidity of B(2) for the borane–N adduct is strengthened. The increase in the Lewis acidity is of advantage to the coordination of aromatic ketone at the B(2) site to form the CTO–borane–ketone adducts. Let us go a step further to study the energy levels of valence natural atomic orbitals (VNAO). As shown in Table III, among the four structures of the CTO–borane adducts, all the VNAO levels of B(2) are positive and the VNAO levels of B(2) for the borane–N adduct **2-1c** are much lower than those for **2-1**, **2-1b**, and **2-1b'**. It is known that when the carbonyl oxygen of aromatic ketone coordinates at the B(2) site to form the CTO–borane–ketone adducts, the interaction between the carbonyl oxygen and B(2) is key to the stability of the adducts. This interaction is in close relationship with the energy differences between the orbital levels of the carbonyl oxygen and B(2). In general, the smaller the energy differences are, the stronger the interaction is. Since the VNAO levels of the carbonyl oxygen of aromatic ketone are negative

(see Table III) and those of B(2) of the CTO–borane adducts are positive, the structure with the smallest energy difference is apparently **2-1c** because it has the lowest VNAO levels of B(2). Furthermore, when aromatic ketone reacts with **2-1c**, it is barely repulsed by the atoms arising from the chair rear of the CTO catalyst with a twisted chair structure because of the long distance between aromatic ketone and the atoms of the chair rear. Therefore, the borane–N adduct **2-1c** is the stablest structure and reacts easily with aromatic ketone to form the CTO–borane–ketone adducts. This result is in correspondence with the calculated formation energies. In addition, it must be pointed out here that when the borane–sulfur adducts **2-1b** and **2-1b'** react with aromatic ketone, aromatic ketone can be repulsed greatly by the atoms arising from the chair rear of the CTO catalyst with a twisted chair structure, which can cause the CTO–borane–ketone adducts to decompose into the borane–sulfur adducts and aromatic ketone. Therefore, the coordination of borane at the S(7) site is of no advantage to the formation of CTO–borane–ketone adducts.

It is seen from Table II that after the formation of the CTO–borane adducts, the B_{BH3}—H_{BH3} bond lengths of the BH_3 moiety are increased considerably. In free borane, the B_{BH3}—H_{BH3} bond length is 1.188 Å. However, the B_{BH3}—H_{BH3} bond lengths for the CTO–borane adducts are **2-1**, 1.197 Å; **2-1b**, 1.202 Å; **2-1b'**, 1.201 Å; **2-1c**, 1.210 Å, and the corresponding overlap populations are 0.417, 0.415, 0.415, and 0.414. It is clear that the formation of the CTO–borane adducts causes the B_{BH3}—H_{BH3} bonds to be weakened. According to the mechanism of catalytic reduction suggested by Corey et al. [5], in the hydride transfer to the carbonyl carbon of aromatic ketone, a hydride arises from the BH_3 moiety. As a result, the coordination of borane with the CTO catalyst **1** is of advantage to the hydride transfer from the BH_3 moiety to the carbonyl carbon. Furthermore, notice that the B_{BH3}—H_{BH3} bond lengths for the borane–N adduct **2-1c** are the longest among the four structures of the CTO–borane adducts, which implies that the B_{BH3}—H_{BH3} bonds of **2-1c** are the weakest.

Now let us turn to the analysis of the stabilization interaction energies $E(2)$ from the second-order perturbative theory [7, 8]. [In the natural bond orbital analysis, $E(2)$ is used to describe the interaction between the donor bond and the acceptor bond of an intramolecule or to describe the delocalization trend of electrons from a donor bond to an acceptor bond.] The selected stabilization interaction ener-

gies $E(2)$ are summarized in Table IV, where BD and BD* represent bonding and antibonding natural bond orbitals, respectively, and LP represents lone pairs. The strength of the B_{BH3}—H_{BH3} bonds is affected by two factors. One is the electron transfer from their bonding orbitals to other antibonding orbitals and the other is the electron acceptance of their antibonding orbitals. The two cases can cause the B_{BH3}—H_{BH3} bonds to be weakened. For all the structures of the CTO–borane adducts, it is seen from Table IV that the stabilization interaction energies $E(2)$ between the B_{BH3}—H_{BH3} bonding orbitals of the BH_3 moiety and other antibonding orbitals are much greater than those between lone pairs and the B_{BH3}—H_{BH3} antibonding orbitals. This result reveals that the tendency of the electron transfer from the B_{BH3}—H_{BH3} bonding orbitals to other antibonding orbitals is primary, which implies that the B_{BH3}—H_{BH3} bonding orbitals tend to be weakened because of the transfer of their bonding electrons to other antibonding orbitals. Furthermore, $E(2)$ for the CTO–borane adducts are much greater than those for borane. It is obvious that the coordination of borane with the CTO catalyst **1** weakens the B_{BH3}—H_{BH3} bonds, which is advantageous for a hydride transfer to the carbonyl carbon of aromatic ketone. In addition, notice that $E(2)$ for the borane–N adduct **2-1c** are the largest among the four structures of the CTO–borane adducts, which implies that **2-1c** has the weakest B_{BH3}—H_{BH3} bonds. As a consequence, the borane–N adduct **2-1c** is of the greatest advantage to a hydride transfer in the enantioselective catalytic reduction.

Conclusions

All the results of this work show that chiral cyclic sulfur-containing oxazaborolidine (CTO) is a twisted chair structure and that the adducts of borane with CTO exist in four plausible structures. In the enantioselective reduction catalyzed by the chiral CTO catalyst, the borane–sulfur adducts may be formed, but they barely react with aromatic ketone to form the CTO–borane–ketone adducts, because they are repulsed greatly by the atoms arising from the chair rear of the CTO catalyst with a twisted chair structure. The borane–N adduct has the largest formation energies and can react easily with aromatic ketone to form the CTO–borane–ketone adducts. The formation of the CTO–borane adducts causes the B_{BH3}—H_{BH3} bond lengths of the BH_3 moiety to be increased and thus enhances the activity of the enantioselective catalytic reduction. Among the four structures of CTO–borane adducts, the borane–N adduct is of the greatest advantage to the hydride transfer from the BH_3 moiety to the carbonyl carbon of aromatic ketone.

References

1. Li, X. S.; Xie, R. G. Tetrahedron: Asymmetry 1996, 7, 2779.
2. Huang, H.-L.; Lin, Y.-C.; Chen, S.-F.; Wang, C.-L. J.; Liu, L.-T. Tetrahedron: Asymmetry 1996, 7, 3067.
3. Reiners, I.; Martens, J.; Schwarz, S.; Henkel, H. Tetrahedron: Asymmetry 1996, 7, 1763.
4. Trentmann, W.; Mehler, T.; Martens, J. Tetrahedron: Asymmetry 1997, 8, 2033.
5. Corey, E. J.; Bakshi, R. K.; Shibata, S. J Am Chem Soc 1987, 109, 5551.
6. Nevalainen, V. Tetrahedron: Asymmetry 1992, 3, 1441.
7. Reed, A. E.; Curtiss, L. A.; Weinhold, F. Chem Rev 1988, 88, 899.
8. Reed, A. E.; Weinstock, R. B.; Weinhold, F. J Chem Phys 1985, 83, 735.
9. Pearson, R. G. J Am Chem Soc 1963, 85, 3533.